Per. Mineral. (2007), 76, 2-3, 241-251 doi:10.2451/2007PM0027
SPECIAL ISSUE: In honour of Ezio Callegari on his retirement http://go.to/permin

PERIODICO di MINERALOGIA
established in 1930

An International Journal of
MINERALOGY, CRYSTALLOGRAPHY, GEOCHEMISTRY, ORE DEPOSITS, PETROLOGY, VOLCANOLOGY
and applied topics on *Environment*, *Archaeometry* and *Cultural Heritage*

On the Palaeozoic Tillite of the Adigrat Group (Tigrai, Ethiopia)

ROSALINO SACCHI [1], MULUGETA ALENE [2 *], MARIO BARBIERI [3] and ANNA CONTI [4]

[1] Dipartimento di Scienze Mineralogiche e Petrologiche, Università degli Studi di Torino, Via Valperga Caluso, 35, 10125, Torino, Italy.
[2] Department of Earth Sciences, Addis Ababa University, P.O.Box 1176, Addis Ababa, Ethiopia.
[3] Dipartimento di Scienze della Terra, Università La Sapienza, Roma,
e Istituto di Geologia Ambientale e Geoingegneria del CNR, Roma.
[4] Unità ISO4, c/o Università degli Studi di Torino, Dipartimento Scienze della Terra

ABSTRACT. — A flat-lying sequence containing diamictite convincingly interpreted as tillites in the literature, occurs at the base of the (Mesozoic) Adigrat Sandstone in the Tigrai Region (Northern Ethiopia). The age of the tillite is controversial, two options (Ordovician and Permian) being put forward by previous authors. As an outcome of petrographic study, the pebbles displayed widespread, previously unreported occurrence of volcanics, thus strengthening the Permian options on the ground of regional geology. Isotopic analyses of C and O allowed comparison with tillites of the underlying, Neo-Proterozoic basement and proved the lack of the extreme excursion of $\delta^{13}C$ that in the Neopoterozoic tillite were seen as supporting the "Snowball Earth" hypothesis for the "Sturtian" age glaciation. Rb-Sr radiometric dating was also performed and yielded results compatible with a Permian age, though facing difficulties connected with intimate intermingling of clasts and matrix, and deuteric alteration.

RIASSUNTO. — Nella regione del Tigrai (Etiopia settentrionale) una sequenza detritica comprendente diamictiti, convincentemente interpretate come tilliti dagli autori precedenti, si interpone tra il basamento neo-proterozoico e la copertura mesozoica. Due datazioni della sequenza si incontrano in letteratura (Ordoviciano *vs.* Permiano). Lo studio petrografico ha dimostrato la estesa presenza di materiale vulcanico, rinforzando la opzione permiana in base a considerazioni di geologia regionale. L'analisi isotopica di C ed O ha riscontrato l'assenza della estrema escursione dei valori di $\delta^{13}C$ che nelle tilliti del basamento hanno fornito supporto alla ipotesi "Snowball Earth". Un tentativo di datazione col metodo Rb-Sr ha incontrato difficoltà costituite dall'intimo mescolamento di materiali diversi (clasti, matrice) e dall'alterazione, ma ha fornito risultati compatibili con un'età permiana.

KEY WORDS: *Ethiopia; Palaeozoic glaciations*

INTRODUCTION AND GEOLOGICAL SETTING

In the Tigrai region (northern Ethiopia), a flat-lying, Palaeozoic, detrital sequence containing diamictites intervenes (Fig. 1) between a late-Proterozoic, low-grade metamorphic basement and the Mesozoic continental deposits known as Adigrat Sandstone (Blanford, 1870). The basement is made of a meta-sedimentary/meta-volcanic sequence folded and weakly metamorphosed, intruded by granites dated at 610 m.y. (see Miller

* Corresponding author, E-mail: mulug@geol.aau.edu.et

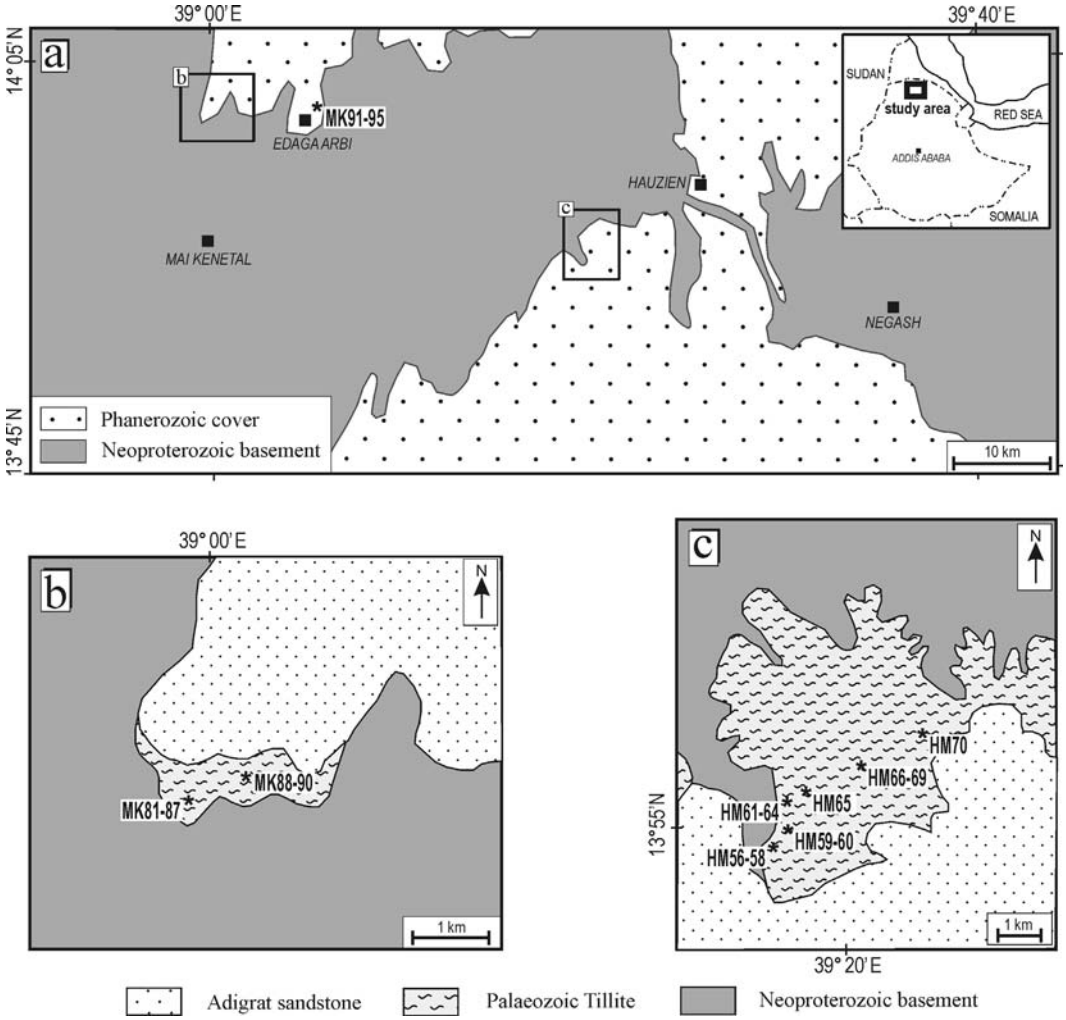

Fig. 1 – Location maps of the tillite-bearing sections (a), of the MK samples (b), and of the HM samples (c).

et al., 2003 and references therein). It is patchily covered by the Palaeozoic sequence over an area of about 2000 sq. km.

The diamictite dealt with in the present paper, recognised by Blanford (1870) and later described by Merla and Minucci (1938), found its modern interpretation, when Dow *et al.* (1971) recognised its glacial nature and suggested an Ordovician age on the ground of lithological similarity with tillites of northern Africa. The dating was subsequently substantiated (Saxena and Assefa, 1983) by admittedly disputable palaeontologic evidence; the alternative correlation being with the well known, widespread, Permian tillites occurring at the base of the Karroo. The dating was, in fact, based on a slow-evolution Coelenterate (*Discophyllum*) whose stratigraphic distribution is also compatible with a late-Palaeozoic age, even though Ordovician-age occurrences are more frequent.

The occurrence of Ordovician tillites in the African continent is well known from the literature. In Ordovician time the South Pole migrated (so to say) from the Libyan Sahara to the Gulf of Guinea (Stampfli and Borel, 2004). On the other hand,

a Permian glaciation is equally well known. So, what is the real age of the Tigre tillites? We will tackle this question in our conclusions on the basis of fresh data.

Dow *et al.* (1971) described two Palaeozoic formations (*Enticho Sandstone* and *Edaga Arbi Tillite*), both connected with a glacial environment and both discordantly covered by the Adigrat Sandstone with a non identifiable chronological gap. Garland (1980) favoured a "close lithological relation" of the three units and thus lumped them into a major "Adigrat Group". He gave a new stratigraphic description of the Palaeozoic terranes, for which he suggested a Permian age as being more likely on the basis of regional geology and palynological indications. The tillites form about 10% of the whole Palaeozoic sequence according to Garland, and were laid down in N-S trending furrows according to Beyth (1972) (which fits well with a Karroo tectonic setting). Dow *et al.* (1971) describe a unit made only of sandstone and conglomerate ("Enticho Sandstone"; thickness <160m) and one rich in tillites ("Edaga Arbi Tillite"; thickness 150-180 m) with boulders up to 6 m in diameter. The tillite bearing unit generally overlies the other one, though the two are often described as "interfingering". The Palaeozoic sequence as a whole overlies the basement with a clear unconformity (see also Alene, 1998, plate 3.7f), whereas a "slight angular unconformity" is tentatively described at the top. Garland (1980) was able to gather thickness data enabling him to build an isopach map of the Edaga Arbi Tillite. As to the Enticho Sandstone, he mentioned its strong variability of thickness and facies.

We cannot but agree with Dow *et al.* (1971, p. 55-56) that the glacial origin of the Edaga Arbi Tillite is "well authenticated". Evidence includes "the massive, almost completely unsorted nature of the deposit; random distribution of megaclasts which are of great variety and reflect faithfully the composition of the provenance; the great size range of the components from fine rock powder to erratic blocks up to 6 m across; presence of boulders known to have travelled large distances [….] ; the remarkably uniform nature of the deposit over hundreds of square kilometres [….] and striking examples of grooves and striations". The glacial origin of the Enticho Sandstone is less obvious, but supported by the bulk of evidence including lithological similarity.

By evaluation of the literature data, a closer look at the lithology of the pebbles was warranted. We thus re-sampled the glaciogenic sequence. Isotopic analyses of the matrix for C and O aimed at palaeo-environmental information allowed a comparison to be made with the tillites of the adjacent Proterozoic basement, the nearest of which - only 30 km away in the "Negash Anticlinorium" - was studied by a research group including some authors of the present paper and referred to the Sturtian Event (Miller *et al.*, 2003). It is well known that the excursion of $\delta^{13}C$, together with other isotopic indicators has lent support to the "Snowball Earth" model , according to which the Neoproterozoic glaciations would have extended to the whole of the Earth surface (references in Miller *et al.*, 2003). An attempt to date these rocks with Rb/Sr method was also performed.

The sampled sections

One of us (M.A.) sampled the Palaeozoic sequence in two sections (Fig. 2) about 40 km away from each other. These we called respectively Hauzien – Megab (HM) and Mai Kenetal – Edaga Arbi (MK). The underlying basement is meta-sedimentary for HM and meta-volcanic for MK. Direct comparison with the "idealized" stratigraphic column built by Garland (1980) was not possible. We thought it necessary to split the MK section (belonging to the Edaga Arbi Unit) into two subsections corresponding to the main part (MK-L) and the top (MK-T), respectively. In the MK-L section, the unsorted texture, the wide size range of the fragments, the random distribution of the pebbles and boulders, are all indications of glacial origin. Some gneissic cobbles must have travelled a long distance, as indicated by their rounded shape and by the nature of the basement. In addition, there are a few striated boulders. Some of these features rule out the alternative hypothesis of a mud flow, as already pointed out by Dow *et al.* (1971). The tillitic features are less displayed both in the HM section (belonging to the Enticho Sandstone) and the MK-T section.

The MK-L sub-section (samples MK 82 to 90) is exposed along the road to Edaga Arbi from the Mai

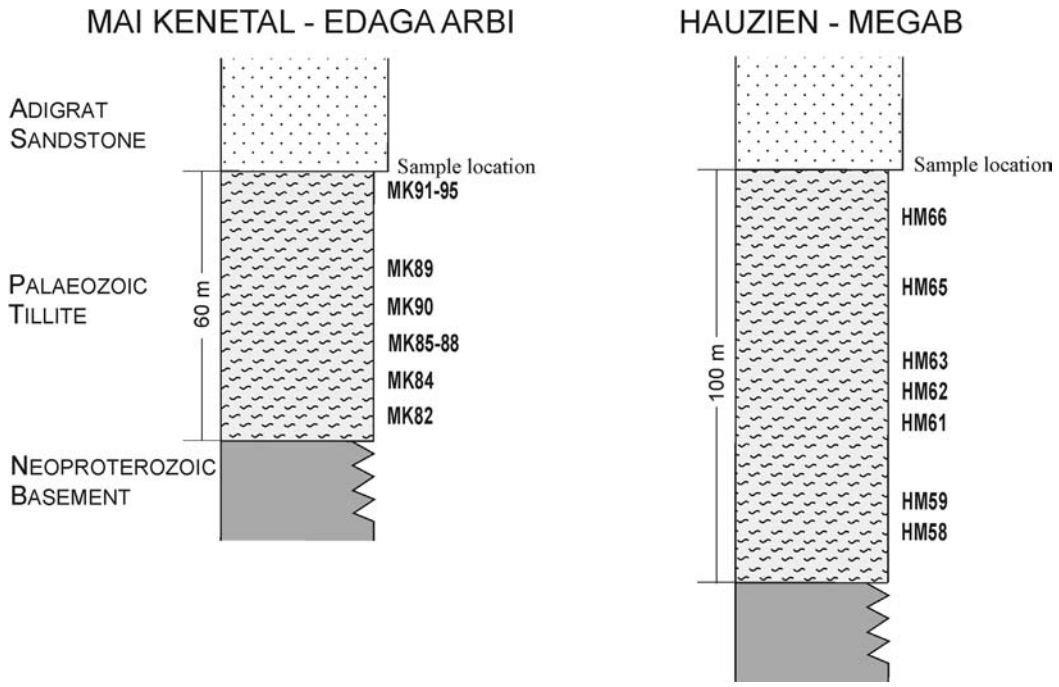

Fig. 2 – Relative position of the samples in the stratigraphic column (see the Appendix for sample description).

Kenetal to Adwa main road, its thickness being about 60 m. Like the HM section, it underlies the Adigrat Formation and overlies the metamorphic basement. Alternating, subhorizontal beds of tillite and sandstone with varying thickness (<10 cm to 2 m) are displayed. Polymict, subrounded, unsorted pebbles and boulders over 1 m in size are common. In thin section, what we see is ill-sorted detrital rocks with a very variable grain size and a matrix of siltstone to quartz-arenite to volcanic ashes with some carbonate. Marked bimodality of clast-size is widespread. In the same sample we find small grains of quartz (diameter: tenths of mm) and larger grains (up to one cm in diameter) with a more varied lithology including volcanics. Also of note besides quartz and feldspar were rock fragments of fine-grained detrital sediments and basement metavolcanics.

The MK-T sub-section (samples MK 91 to 95), corresponding to the topmost part of the sequence is met right in the centre of the small town called Edaga Arbi after which the name of the formation was derived. A problematic pinkish to yellowish-brown conglomerate with felsic-looking, well-sorted and variably rounded pebbles, exposed over a thickness of 30 to 40 m, displays the appearance of water- rather than ice-deposited sediment. In thin section, this sequence turned out to be composed of a mixture of quartz-arenite with volcanic material, the latter forming discrete volumes large enough for selective analysis.

The HM section (samples 58 to 70) is located about 15 km SW of Hauzien along the Megab-Koraro dry-weather road. The exposed thickness is over 100 m. The unit underlies Jurassic sandstone belonging to the Adigrat Sandstone formation and it has an unconformable contact with the underlying metamorphic basement. It contains varying thickness of sub-horizontal sandstone and siltstone beds. The supposedly tillite beds (brownish, yellow, grey in colour) display a poorly sorted matrix containing polymict gravels with sub-rounded pebbles and boulders of granite, meta-volcanics, slate, gneiss and quartz. These beds are frequent in the lower and upper parts of the section, whereas in the middle part, well laminated (often highly weathered and friable) siltstone and sandstone are widespread. In thin section the rocks display a

variable amount of silty to quartz-arenitic matrix. The clasts include volcanics, quartz, basement material (mainly slates, but also grains of granite minerals such as feldspar, zircon and tourmaline), and glass of uncertain origin and fragments of detrital rocks. The grain-size frequency curve is bimodal, though less markedly so than in MK-L. The bulk of these features is thus suggestive of non-first-cycle sedimentation. Altogether, volcanic material is relatively unfrequent in the HM sequence, which accounts for our choice of analyzing mainly MK samples.

A description of the samples is given in the Appendix.

Measurements of $\delta^{13}C$ and $\delta^{18}O$

Eleven samples, out of twenty, have been analysed for C and O isotopic composition. The majority of samples (8 out of 11) come from the MK-L section, whereas HM turned out to have a matrix with scanty carbonate, if at all (at variance with Beyth, 1972, p. 94).

Methodology

Samples were cleaned of external contaminants using a trim saw, then crushed in an agate mortar and pestle to obtain powder. Stable isotopes (C and O) compositions were determined on the bulk carbonate sample fraction by the classic method (Mc Crea, 1959) in which carbonate powder reacts in a vacuum with 100% phosphoric acid at 25°C. Isotope ratios were determined with a Finnigan MAT 250 mass spectrometer (Department of Earth Sciences, University of Turin) and are reported relative to the PDB standard. Analytical uncertainties are ~0.10 per mil for $\delta^{13}C$ and $\delta^{18}O$.

Results

Stable isotopes ratios are reported in Table 1 and Fig. 3. All the samples turned out to be low in ^{13}C e ^{18}O. As regards carbon, a pattern of variation is not detectable, whereas the range of values is of some interest. The most "tillitic" section (MK-L) displays negative values of $\delta^{13}C$ with a range of 4 per mil (-2 to –6); definitely devoid of the extreme values typical of the Neo-Proterozoic tillites from the literature including the adjacent one studied by Miller *et al.* (2003). The typical evolution of $\delta^{13}C$, with positive values at the base of the glaciogenic sequence is lacking (as is the "carbonate cap"). Altogether, there is a distinct lack of the features which triggered the birth of the Snowball Earth model.

The $\delta^{13}C$ values yielded by our analyses are fairly common as the outcome of diagenesis of a sediment in a sub-aerial environment. The "most negative" value is in the range normally displayed by meteoric and aquifer waters. As regards volcanics-rich sequence HM, the occurrence of "less negative" values is compatible with an addition of heavy isotope from deep sources, and thus not unexpected.

Diagenesis would seem to account also for low $\delta^{18}O$ values, although interaction with a low-$\delta^{18}O$ metamorphic basement cannot be ruled out as a joint cause.

Sr, Rb and $^{87}Sr/^{86}Sr$ determinations

The hitherto unknown volcanic nature of the clasts and part of the matrix is of indirect chronological value as discussed in the conclusions. This prompted Rb/Sr investigation on volcanic clasts and matrix.

Methodology

A limited number of samples were selected for isotopic analysis. These were selected among rocks containing the best preserved clasts of volcanic material. Macroscopically, volcanic clasts consist of variably rounded, sometimes elliptical fragments, often with an oxidised rim. Texture of these samples has been described previously. As each sample is lithologically heterogeneous, care was taken to analyze the different portions separately with special attention given to the distinction of matrix and clasts (see Table 1). For this purpose a drilling technique was used and the powders used for isotopic analyses were taken from the most internal part of each volcanic clasts and from the matrix. Both volcanic clasts and the enclosing matrix were sampled (grey colour in macroscopic samples). Two whole rocks were also analysed.

As previously reported (see MK lithology in the Appendix), some samples contain variable amounts of Ca carbonate, which is clearly of secondary origin. To get rid of this component, the drilled powders were leached with a solution of HCl 0,2 N, and subsequently washed with bidistilled water.

For the chemical and isotopic analyses, 1 g of weighed, powdered sample has been etched with HF + HNO_3 and the residue diluted to 100 ml volume with bidistilled water. An aliquot of the above solutions was used to detect, through IC plasma, the concentrations of Sr and Rb. The $^{87}Sr/^{86}Sr$ ratios have been determined by a VG 54E mass spectrometer. The $^{87}Sr/^{86}Sr$ ratios measured were normalised to $^{87}Sr/^{88}Sr$ of 0.1194 and are reported relative to the NBS 987 standard = 0.71024±2.10^{-5} (as 2σ). All the isotopic ratios are within an error, expressed as 2σ, of ±2.10^{-5}.

Results

The measured $^{87}Sr/^{86}Sr$ isotope ratios and Rb and Sr abundances are given in Table 1 and the plot of $^{87}Rb/^{86}Sr$ *vs.* $^{87}Sr/^{86}Sr$ in Fig. 4. The data show variable compositions for the analysed materials.

TABLE 1

Sr and Rb (ppm), Rb-Sr isotopic compositions of analysed samples, $\delta^{13}C$ and $\delta^{18}O$ values of calcite referred to the PDB and SMOW standards (see text for analytical precision), and geographic coordinates.

sample	Sr	Rb	$^{87}Rb/^{86}Sr$	$^{87}Sr/^{86}Sr$	$\delta^{13}C$ *vs.* PDB	$\delta^{18}O$ *vs.* PDB	$\delta^{18}O$ *vs.* SMOW	latitude	longitude
MK 82 wr	-	-	-	-	-6.26	-3.63	27.12	N14º 02' 05"	E38º 59' 42"
MK 84 wr	-	-	-	-	-3.5	-5.39	25.30	N14º 02' 05"	E38º 59' 42"
MK 85 wr	-	-	-	-	-2.69	-6.11	24.56	N14º 02' 05"	E38º 59' 42"
MK 86 wr	148	149	2.91	0.7135	-2.44	-2.54	28.24	N14º 02' 05"	E38º 59' 42"
MK 87 bas	154	150	2.82	0.72623	-	-	-	N14º 02' 05"	E38º 59' 42"
MK 87 g	50	43	2.49	0.7119	-2.86	-6.12	24.55	N14º 02' 05"	E38º 59' 42"
MK 88 wr	96	93	2.8	0.71313	-4.43	-5.36	25.33	N14º 02' 13"	E39º 00' 07"
MK 89 wr	-	-	-	-	-4.61	-4.63	26.09	N14º 02' 13"	E39º 00' 07"
MK 90 wr	-	-	-	-	-2.85	-1.74	29.07	N14º 02' 13"	E39º 00' 07"
MK 92 g	71	33	0.82	0.70526	-	-	-	N14º 02' 21"	E39º 04' 05"
MK 92 v	59	16	0.79	0.70511	-	-	-	N14º 02' 21"	E39º 04' 05"
MK 93 g	114	68	1.72	0.70884	-	-	-	N14º 02' 21"	E39º 04' 05"
MK 93 v	106	69	1.88	0.70948	-	-	-	N14º 02' 21"	E39º 04' 05"
MK 94 v	47	12	0.74	0.7119	-	-	-	N14º 02' 21"	E39º 04' 05"
MK 94 g	42	<1	-	0.71048	-	-	-	N14º 02' 21"	E39º 04' 05"
MK 95 v	59	38	1.86	0.70939	-	-	-	N14º 02' 21"	E39º 04' 05"
MK 95 g	127	86	1.96	0.70979	-	-	-	N14º 02' 21"	E39º 04' 05"
HM61 wr	-	-	-	-	-0.52	-1.48	29.33	N13º 55' 07"	E39º 19' 33"
HM63 wr	-	-	-	-	-1.2	-4.92	25.79	N13º 55' 07"	E39º 19' 33"
HM65 wr	-	-	-	-	-1.56	-2.47	28.31	N13º 55' 16"	E39º 19' 46"

bas: fragment of basement rock, g: ground-mass, v: juvenile volcanic clast, wr: whole rock.

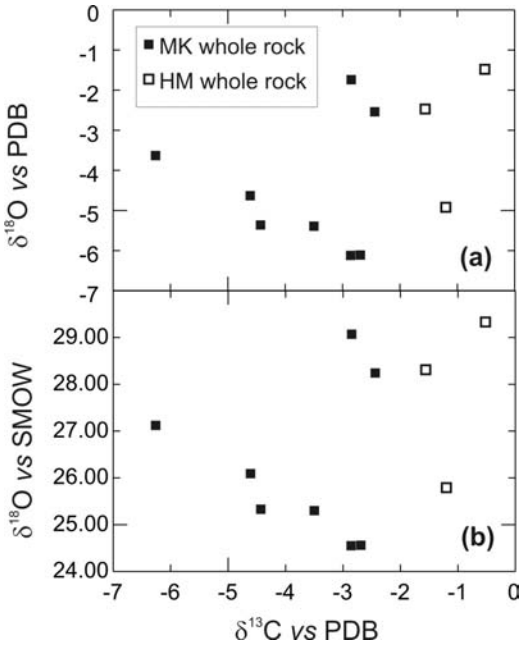

Fig. 3 – Plot of $\delta^{13}C$ *vs.* $\delta^{18}O$ values; $\delta^{18}O$ is plotted *vs.* PDB and *vs.* SMOW in (a) and (b), respectively. Calcite from HM section shows a lesser depletion in ^{13}C, while $\delta^{18}O$ values span widely. Data from MK section are generally displaced

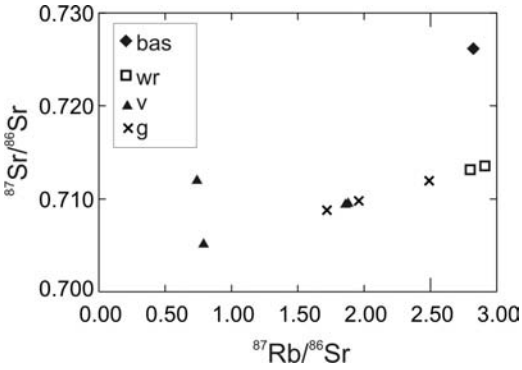

Fig. 4 – $^{87}Rb/^{86}Sr$ *vs.* $^{87}Sr/^{86}Sr$ diagram for the analysed samples; bas: fragment of basement rock, g: groundmass, v: juvenile volcanic clast, wr: whole rock. If RS-87-bas and RS-94 are excluded (see discussion in the text), the resulting

In general, portions coming from the same rock have similar isotopic and Rb and Sr values, except for sample MK87, in which the matrix (MK-87-g) shows much lower $^{87}Sr/^{86}Sr$ than the supposedly volcanic clast (MK-87-bas). MK-87-bas could have suffered modification of $^{87}Sr/^{86}Sr$ ratio by deep alteration.

As to Fig. 4, except for MK-94 and the clast MK-87-bas, the bulk of the analysed samples fit a perfect positive trend (r = 0.99), whose intercept with vertical axis is at $^{87}Sr/^{86}Sr = 0.70199$. Both volcanic clasts, the surrounding matrix and some whole rocks plot on this line. If considered as an isochron curve, the array of data would yield an age of 279.3 Ma with an initial Sr isotopic ratio as low as 0.701990, a dating consistent with the presence of volcanic clasts, as discussed earlier.

However, the hypothesis that the obtained trend is an isochron conflicts with a number of problems. First of all, the correlation has an exceedingly high least squares regression coefficient (r = 1). This is at odds with rocks that have suffered variable degrees of alteration. Also the initial Sr isotopic ratios are too low, even for magmas representing very primitive mantle derived melts. Moreover, magmas with these values would have much lower Rb contents than those observed in analysed volcanic clasts. Therefore, we believe that the linear trend defined by the bulk of the analysed samples may represent a mixing line between juvenile volcanic material and the matrix. This is supported by the fact that the two whole rocks analysed (MK-86-wr and MK-88-wr, both containing little juvenile material) plot at the upper end of the trend, whereas samples consisting almost entirely of volcanic clasts (e.g. MK-92-v) plot at the opposite end of the line. In principle, mixing may be an effect of interaction of magmatic fragments and matrix during eruption, or may also be an artefact of the sampling technique that was unable to separate matrix from volcanic clasts during drilling because of the intimate intermingling between clast and matrix observed in this section.

If the observed trend is a mixing line, it should be concluded that it has no geochronological significance. However, the hypothesis that the detritic matrix end-member had similar or only slightly higher initial Sr isotopic value to the volcanic material with which it intermingled cannot be discarded if we consider that most of the fine-grained material of the detritic clasts are surrounded by a fine-grained matrix consisting of juvenile volcanic ash. This lends support to the conclusion

that the Lower Permian age indicated by Rb/Sr *vs.* $^{87}Sr/^{86}Sr$ data can be taken as broadly correct.

CONCLUSIONS

In spite of the limited amount of field material and information, some results are of value, and warrant further research.

i) In thin section, the clasts of the Palaeozoic sequence exhibit some fine grained sedimentary rocks being remnants and witness of a pre-glacial post-Proterozoic sequence which did not escape erosion. A polycyclic nature of the Palaeozoic tillite-bearing sequence is also indicated by its bimodality suggesting derivation from a detrital sequence rather than a basement.

ii) A common feature (particularly well displayed in the samples from the MK section) is the widespread presence of volcanics in the sequence, especially the larger clasts. Some samples are entirely composed of pyroclastic material.

Microscopic and mesoscopic observation suggests that the analysed samples consist mainly of volcanic clasts bound by a partly volcanic matrix. Among volcanic clasts, some are porphyritic and strongly altered (e.g. in samples MK-87, MK-88) and probably represent lithic material from earlier volcanic phases. Others are optically isotropic with rare phenocrysts of feldspars and sometimes clinopyroxene. These show oxidised border and irregular margins with the matrix. In some cases crystals from the matrix are enclosed inside the volcanic clast. These textural features indicate that the isotropic material represents juvenile magma fragments that intermingled with the matrix when both were in a plastic state. This leads us to conclude that the rocks under consideration were formed by eruption of magmas into an unconsolidated sediment including a variable proportion of juvenile volcanic ashes. The oxidised rims of the volcanic clasts probably represent a quenched border formed when juvenile scoriae went in contact with wet unconsolidated sediments. Overall, the process is similar to those suggested for the formation of peperite. The environment could be marine or continental, including the base of a glacier (e.g. Batiza and White, 2000; Smellie, 2000).

As regards the presence of well recognisable volcanics in the pebbles, it may sound surprising that such an important feature was never reported in the literature. Deuteric alteration makes the rock of the pebbles difficult to recognise in a hand specimen. On the other hand, a petrographic analysis of the pebbles was never mentioned in the literature, and it looks as though it was never performed. It also looks as though we are dealing here with the casual convergence of the action of two agents, both able to produce diamictites, namely glaciers and volcanoes, which obviously blurred the picture.

The two sequences (HM and MK), referred to the same unit, and made of apparently similar coarse grained sediments, displayed some differences in the lithology of the clasts. This heterogeneity can hardly be explained in the absence of a detailed survey.

The problem of the age of the tillites (Ordovician *vs.* Permian) was left unanswered by Beyth (1972), whereas Garland (1980) favoured the Permian option for a sum of indications as mentioned here in the opening section. The Permian option is much strengthened by the volcanic material. Whereas volcanic activity in Ordovician time is regionally unknown, the Permian of southern and eastern Africa preserves widespread evidence of volcanic activity connected with early phases of the Pangea breakup. Tensional tectonics goes along well with the low value of $^{87}Sr/^{86}Sr$ I.R.

ACKNOWLEDGEMENTS

R.S. spent a great many hours in the microscope lab with Ezio Callegari, Evelina Giobbi Mancini, e Giangaspare Zuffa: a warm thank is due to all of them. Angelo Peccerillo read the ms. critically and gave precious advice on the interpretation of the Rb-Sr data. Luca Martire kindly read an early draft of the paper and supplied constructive criticism. The analyses of Rb and Sr were performed in the Istituto di Geologia Ambientale e Geoingegneria, CNR, Roma; those of O and C in the ISO4 Unit, c/o Dipartimento di Scienze della Terra, Università degli Studi di Torino. M.A. gratefully acknowledges support from the ORGP, Addis Ababa University (research grant RPO/GF/1995ec/008).

Appendix

The samples, listed in their stratigraphic order (starting from the top) are described hereafter. When "bimodality" is mentioned, the size *vs.* frequency curve is referred (a frequent feature, as we will see).

HM Section

HM 66. Detrital rock with a chaotic texture, a fine grained, clear to rusty matrix, two classes of clasts (bimodality) with an average diameter of 0.1 and >1 mm respectively. The bigger clasts, rare and rounded and all made of quartz, have a variable size and irregular distribution. Grains of zircon, tourmaline and hornblende suggest a contribution from the basement.

HM 65. Fine-grained sandstone (locally a siltstone) with rare calcite. Composition of the clasts: cm-size grains of a very-fine-grained sedimentary rock; rare grains of a pyroclastic material, with a weak optic anisotropy; euhedral crystals made of epigenetic calcite; arenite, chert, feldspar turned into kaolin.

HM 63. Fine-grained sandstone passing into a siltstone with a well displayed bedding. A fine grained matrix with clasts of 0.05 mm. Rare granules of 0.5 – 1 mm are made of quartz, very-fine-grained volcanics with rare phenocrysts, volcanic glass and very rare K-feldspar.

HM 62. Sandstone from a heterogeneous source. Average grain size: 0.2 mm. Composition of the clasts: mainly quartz, but also shales and minerals from the basement (microcline, plagioclase, mica).

HM 61. Ill-sorted, well-bedded sandstone with granules of a highly variable size in a scanty, rusty matrix of kaolin and carbonate. Clasts diameter is generally 0.2 mm. Bigger (1 mm) granules are made of quartz and (more rarely) alkali feldspar, fine grained volcanics (probably a tuff) rich in sericite, a euhedral mineral altered into carbonate, some dubious (preudomorphosed) mafic mineral and (dubious) meta-volcanics from the basement. Strong bimodality.

HM 59. Quartz-arenite. Scanty, clayey to silty matrix with clasts 0.4 mm in diameter on average. Clast composition: quartz with rare glass.

HM 58. Sandstone with a rusty, pelite matrix. Clast composition: quartz, slates, dolomite, feldspar (plagioclase and microcline), fragments of an acidic metamorphic rock, and fragments of a porphyritic rock with phenocrysts of plagioclase and an unidentifiable mineral with low birefringence (a feldspathoid?). Clasts (making up 2/3 of the rock): diameter c. 1 mm with one (alkali-feldspar) grain of 5 mm.

MK Section

MK 95. Largely made of volcanic clasts surrounded by a matrix made of fine grained material, mostly volcanic ashes and a few detrital minerals, especially quartz and accessory zircon. Volcanic clasts are rounded and appear isotropic with a few microphenocrysts of feldspar at the microscope. They have lobate interface with the matrix, and show somewhat more dense texture and stronger oxidation at rims.

MK 94. Highly heterogeneous rock made of quartz-arenite, with rounded volcanic clasts about 1 cm in diameter set in a detrital matrix made of crystals of quartz, feldspar and accessory zircon and tourmaline separated by a fine grained, brown, optically isotropic matrix, most probably representing volcanic ashes. Larger volcanic clasts sometimes enclose small amounts of detrital minerals from the matrix. Their margins are oxidised and show somewhat denser structure than the internal of the clasts that show a shard-like, fragmented texture. At the microscope, volcanic clasts appear isotropic with a few phantoms of feldspar phenocrysts, indicating an original poorly porphyritic glassy texture.

MK 93. Rounded pebbles (diameter 1 to 2 cm) of isotropic volcanic glass float in a quartz-arenite made of 0.5 mm quartz grains with a scanty (c. 10%) brownish, semi-opaque, optically isotropic matrix. Interface between volcanic clasts and matrix is irregular and the margins of volcanic clasts are oxidised and locally "indented" by the quartz grains of the arenite.

MK 92. The rock is largely made of optically anisotropic volcanic material with clasts 0.5 to 1 cm in diameter (bound by a fine grained matrix) with infrequent, very small grains of quartz. A weak cleavage affects both matrix (more markedly) and pebbles. Cross-cutting, flat veins

of a non-identifiable low-birefringence material with a somewhat fibrous texture. An oxidised border, visible both at the microscope and in hand specimens, is present in the volcanic clasts.

MK 91. The rock is wholly made of glassy volcanic material embodying small (0.02 to 0.2 mm) non-rounded grains of quartz. A quasi-isotropic, very-fine-grained tuff matrix is mixed up with volcanic clasts yielding an overall chaotic texture. A dark pigment locally highlights a weak cleavage

MK 89. Alternating beds of (i) fine-grained quartz-arenite and (ii) greywacke. The quartz-arenite of beds (i) contains scattered, larger, sub-angular grains of plagioclase and K-feldspar. The greywacke (ii) displays a fine-grained fraction similar to the quartz-arenite (i), with a bimodal grain-size frequency curve (peaks at 0,2 and c. 2 mm, respectively). It also contains larger (some mm in size) sub-angular fragments of rocks, namely volcanics, reddish shales, and shreds of porphyric lava looking like “soft” pebbles. Some carbonate in the matrix.

MK 90. A mesh of sub-angular, often euhedral, feldspar grains forming a sort of grit. Feldspar, usually altered, may display a Karlsbad-type twinning. A part of it is identifiable as plagioclase. Aggregates of clear, non-altered grains with some mica are also present, as well as angular grains of downgraded, mafic minerals.

MK 88. Arenite with a bimodal grain-size frequency curve: the large grains (c. 1 cm) being made both of basement rocks and volcanics, the small grains mainly of quartz. The volcanic material shows different texture and composition than observed in other samples. It is altered and porphyritic. Some of these clasts are rich in phenocrysts of plagioclase and quartz embedded by a groundmass of tiny feldspar prisms; others are partly re-crystallized glass with rare, unidentifiable phenocrysts. The basement material includes (i) fragments of microcline, microcline-perthite, and (ii) metavolcanics made of sericite-rich beds and deformed grains of plagioclase with re-crystallized quartz and plagioclase in pressure shadows.

MK 87. Ill-sorted, heterometric arenite with bimodal grain size (mm 0.1 and mm 2 plus matrix and a few 1 cm grains). The fine grained fraction is mainly quartz set in a finer-grained, optically isotropic matrix. The coarse grained fraction includes a variety of rocks and minerals: (i) phenocrysts of altered feldspar with a Karlsbad-type twinning; (ii) volcanics with flow structures and phenocrysts of K-feldspar, plagioclase and quartz; (iii) volcanics with interwoven, tiny plagioclase prisms and rare phenocrysts of an altered, unidentifiable coloured mineral; (iv) basement meta-volcanics; (v) quartz; (vi) epigenetic calcite. Calcite also occurs as rims around some of the large grains.

MK 86. Rock with a bimodal grain-size frequency curve (peaks at mm 0.4 and 5, plus matrix). The small grains are mainly quartz. The large ones - though mainly volcanic - include a variety of other materials: basement granitoids, plagioclase, a feldspar with Karlsbad-type twinning, epigenetic calcite and euhedral, altered mafic minerals. The grains of volcanics include:

- a glassy, ore-rich rock with flow structures with phenocrysts of plagioclase and alkali feldspar;
- a rock with micro-crystalline ground mass and phenocrysts of plagioclase.

MK 85. Coarse grained, heterometric sediment with abundant calcite in the matrix. Grain-size frequency curve is bimodal with peaks at 0.3 and >3 mm, respectively. The small grains are quartz, the large ones volcanic, namely:

- a very-fine-grained rock with tiny, unidentifiable phenocrysts and fragments of partly re-crystallized glass;
- a rock with a groundmass made of tiny plagioclase prisms, displaying flow structures
- a rock with plagioclase and sanidine phenocrysts set in a groundmass made of partly recrystallized glass;
- a problematic, acidic metamorphic rock, apparently a meta-granite (not known to occur in the basement).

MK 84. Fine-grained bedded detrital sediment. The grain-size frequency curve is bimodal with peaks at mm 0.1 and 1, respectively. The grains, mostly lithic, set in a rusty-looking, carbonate-rich matrix, display various lithologies including: slates, very-fine-grained detrital material (tuff?), feldspar (microcline and plagioclase) and (dubious) basement meta-volcanics. A certain amount of flattening of the large grains outlines a planar anisothropy parallel to the bedding.

MK 82. Detrital, heterometric, crudely layered sediment displays the usual, bimodal grain-size

frequency curve with peaks at mm 0.5 and 0,1, plus a rusty-looking finer-grained matrix. Grains are quartz, rare K-feldspar, plagioclase, rare slate and some altered euhedral crystals of an unidentifiable phase.

REFERENCES

ALENE M. (1998) – *Tectonomagmatic evolution of the Neoproterozoic rocks of the Mai Kenetal – Negash area, Tigrai, northern Ethiopia*. Ph.D. Thesis, University of Torino, 140 pp.

BATIZA R. and WHITE J.D. (2000) – *Submarine lavas and hyaloclastites*. In Sigurdsson H. (Ed.) *Enciclopedia of volcanoes*, Academic Press, N.Y., 361-381.

BEYTH M. (1972) – *The geology of central and western Tigre*. Ph.D. Thesis, University of Bonn, 155 pp.

BLANFORD W.T. (1870) – *Observations on the Geology and Zoology of Abyssinia*. Mcmillan & Co., London, 487 pp.

DOW D.B., BEYTH M. and TSEGAYE H. (1971) – *Palaeozoic glacial rocks recently discovered in northern Ethiopia*. Geol. Mag., **108**, 53-59.

GARLAND C.R. (1980) – *Geology of the Adigrat area*. Ministry of Mines, Addis Abeba, Memoir n. 1, 51 pp.

MC CREA J.M. (1950) – *On the isotope chemistry of carbonates and a paleotemperature scale*. J. Chem. Phys., **18**, 849-857.

MERLA G. and MINUCCI E. (1938) – *Missione Geologica nel Tigrai*. Reale Accademia d'Italia, Roma, 319 pp.

MILLER N.R., MULUGETA A., SACCHI R., STERN R.J., CONTI A., KROENER A. and ZUPPI G. (2003) – *Significance of the Tambien Group (Tigrai, N. Ethiopia) for the Snowball Earth events in the Arabian-Nubian Shield*. Precambrian Res., **121**, 263-283.

SAXENA G.N. and ASSEFA G. (1973) – *New evidence on the age of the glacial rocks of northern Ethiopia*. Geol. Mag., **120**, 549-554.

SMELLIE J.L. (2000) – *Subglacial eruptions*. In: Sigurdsson H. (Ed.), Enciclopedia of volcanoes, Academic Press, N.Y., 403-418.

STAMPFLI G.M. and BOREL G. (2004) – *The TRANSMED transects in time and space*. In: Cavazza W. *et al.* (Eds.), The Transmed Atlas: the Mediterranean Region from crust to mantle. Springer V., Berlin, 53-80.